V1 neurons encode the perceptual compensation of false torsion arising from Listing's law

Mohammad Farhan Khazali[a,1], Hamidreza Ramezanpour[a,2], and Peter Thier[a,3]

[a]Hertie Institute for Clinical Brain Research, Department of Cognitive Neurology, University of Tübingen, 72076 Tübingen, Germany

Edited by Michael E. Goldberg, Columbia University, New York, NY, and approved June 16, 2020 (received for review April 25, 2020)

We try to deploy the retinal fovea to optimally scrutinize an object of interest by directing our eyes to it. The horizontal and vertical components of eye positions acquired by goal-directed saccades are determined by the object's location. However, the eccentric eye positions also involve a torsional component, which according to Donder's law is fully determined by the two-dimensional (2D) eye position acquired. According to von Helmholtz, knowledge of the amount of torsion provided by Listing's law, an extension of Donder's law, alleviates the perceptual interpretation of the image tilt that changes with 2D eye position, a view supported by psychophysical experiments he pioneered. We address the question of where and how Listing's law is implemented in the visual system and we show that neurons in monkey area V1 use knowledge of eye torsion to compensate the image tilt associated with specific eye positions as set by Listing's law.

eye movement | visual perception | orientation discrimination | V1 | Listing's law

We explore a visual scene by a sequence of saccades and brief moments of fixation. According to Listing's law (1), the movements of our eyes from one position to the next are rotations around an axis that lies in a plane, whose orientation relative to the head is determined by the starting position of the eyes (2). In the specific case of the eyes starting from straight ahead, i.e., from the primary position, this plane has a frontoparallel orientation and is usually referred to as Listing's plane. The consequence of this principle is the emergence of an amount of torsion of the eye around the line of sight (false torsion) that is a function of the horizontal and vertical deviation from straight ahead, independent of the starting position of the eyes (1–3). The amount of false torsion is zero for fixation positions on the horizontal and vertical head-centered meridians and significant for positions on or close to the diagonals where it grows with eccentricity (*SI Appendix*, Fig. S1). For instance, fixating at (35°, 35°) will be accompanied by around 15° of clockwise false torsion relative to the primary position. Although the false torsion will inevitably rotate the image on the retina and thereby rotate the world vertical relative to the retina vertical, we do not perceive a tilting world and, in general, are not aware of any retinal consequences of this eye torsion (2, 4). Based on afterimage experiments (2), Hermann von Helmholtz, to whom we owe the detailed elaboration of Listing's law, could show that this is a consequence of a perceptual reinterpretation of the image orientation, based on knowledge of the amount of false torsion (4–7). It is the integration of this torsion prior into the perceptual interpretation of retinal images that allows us to ensure the stable perception of object and world orientation when exploring visual scenes. Here we show that the perceptual interpretation is taking place in area V1 as its neurons exhibit orientation preferences and receptive field (RF) positions that are invariant to the retinal consequences of false torsion.

Results

Monkeys' Perception Accounts for False Torsion. We wanted to know where and how information on false torsion is integrated into the processing of the retinal image in the visual system at the level of single neurons. To answer this question, we resorted to macaque monkeys as they explore scenes like humans, shifting fixation from one position to the next, therefore burdening also their visual system with false torsion-based image rotations (8–11). To clarify whether they are able to perceptually compensate the resulting retinal image tilt like humans, we trained two monkeys (M1 and M2) on a two-alternative forced choice task in which they had to decide whether a slim line (7° visual angle length originating from the fixation dot with width of 0.8°) was tilted clockwise (cw) or counterclockwise (ccw) relative to the external world-centered vertical with the head immobilized upright via an implanted head post (Fig. 1*A*). The line whose tilt was randomly selected from a set of tilt angles (method of constant stimuli) was present during 1-s periods of stable fixation (eye position within a window of 1° × 1°). After this period both the line and the fixation dot disappeared and two response targets, one on the left and the other one on the right side appeared, prompting the monkeys to saccade to the right in the case of perceived cw tilt and to the left for perceived ccw tilt. To facilitate understanding the behavioral requirements, we added a visual reference line aligned with the world vertical in the early phase of the behavioral training (for details see *Materials and Methods*). In these "training trials," the monkeys quickly attained a high and reliable level of performance: Whenever the tilt

Significance

Eye movements have three degrees of freedom, the ability to move horizontally, vertically, and torsionally. Eye movements serving the fovea strictly control eye torsion. The amount of torsion associated with a particular eye position is specified by Listing's law. Because of prior knowledge of the torsion set by Listing's law, we perceive the world as upright although its retinal image may be tilted by varying degrees. We first show that also monkeys use a torsion prior to ensure a veridical perceptual reinterpretation of image tilt. We then demonstrate that this reinterpretation is a consequence of the fact that V1 neurons use the torsion prior to adjust their orientation preferences and to reposition their receptive fields relative to the retina.

Author contributions: P.T. developed the conceptual framework of the research; M.F.K. and P.T. designed the study; M.F.K. and H.R. collected and analyzed the psychophysics data; M.F.K. collected and analyzed the neurophysiological data; M.F.K., H.R., and P.T. discussed the experimental results; and M.F.K. and P.T. wrote the paper.

The authors declare no competing interest.

This article is a PNAS Direct Submission.

Data deposition: Data for this article have been deposited in Figshare, https://doi.org/10.6084/m9.figshare.12159537.v1

[1]Present address: Center for Neural Science, New York University, New York, NY 10003.

[2]Present address: Centre for Vision Research, York University, Toronto, ON M3J 1P3, Canada.

[3]To whom correspondence may be addressed. Email: thier@uni-tuebingen.de.

This article contains supporting information online at https://www.pnas.org/lookup/suppl/doi:10.1073/pnas.2007644117/-/DCSupplemental.

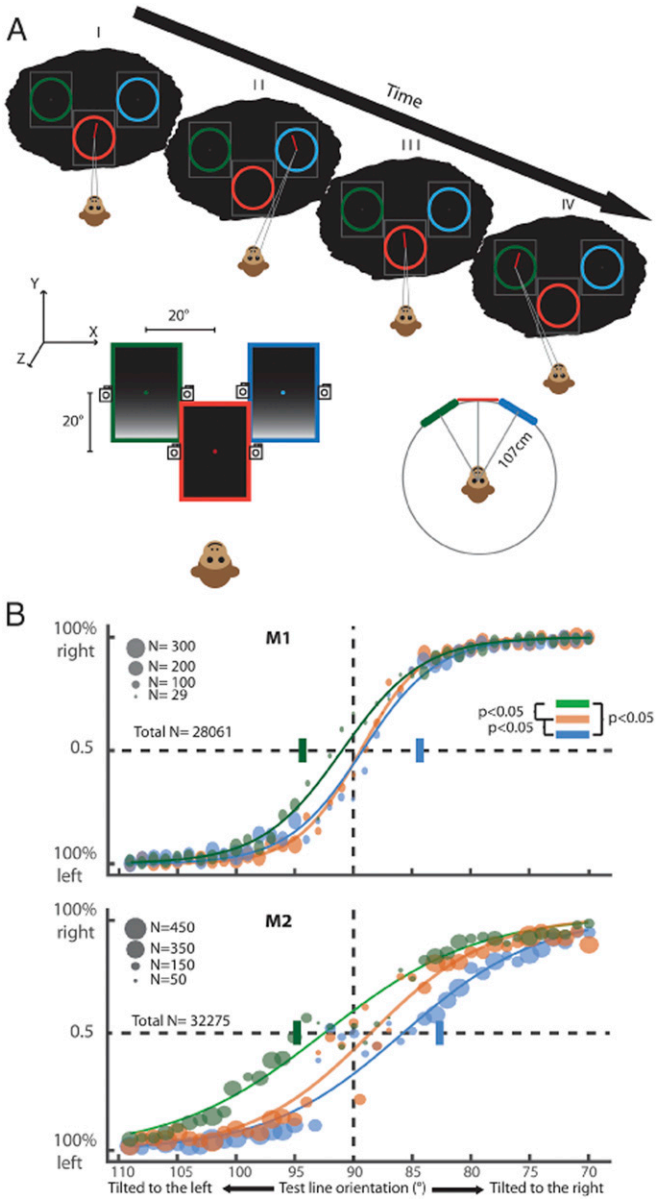

Fig. 1. Assessing the subjective visual vertical of monkeys for different gaze directions. (*A*) *Lower* illustrations: The monkey fixated on a target presented in the center of three monitors arranged tangentially on a 107-cm radius sphere with the monkey in the center of the sphere. One of the monitors was positioned straight ahead (0°, 0°) and the two others were positioned in the upper right (20°, 20°) and the upper left (−20°, 20°) position, respectively. Each monitor was equipped with two cameras, one facing the left eye and the other one the right eye, providing eye snapshots used to determine the amount of false torsion. *Upper* illustration: Sequence of psychophysical tests in a typical daily experimental session probing a monkey's SVV. The fixation target appeared on one of the three monitors and the monkey had to report the orientation of the test line relative to a vertical reference line (not shown) or relative to his internal reference (i.e., the SVV) by making an indicative saccade at the end of a trial. At the end of a block of trials the target and the test line jumped to another monitor. Note that a black circular aperture (indicated by the colored circles) covered the monitor edges (indicated by the gray rectangle) to eliminate any external orientation cues. (*B*) Plots of monkey M1 and M2 decisions on the orientation of the test line (in the absence of a visual reference) as a function of the true test line orientation. The plots are based on all daily experimental sessions including around 28,000 trials for M1 and 32,000 trials for M2. The colors distinguish data for the three monitors/gaze directions (green, upper left monitor; blue, upper right; red, central). The chance-level point (50% right vs. left choices, the PES) was taken as a measure of a monkey's SVV. Note that the SVV for the upper left gaze direction is shifted slightly in a counterclockwise direction and that for the upper right gaze direction is in a clockwise direction with respect to the SVV for the central gaze direction. The SVV differences between gaze directions are minimal for M1 and relatively larger for M2 compared to the changes in false torsion. The short vertical green and blue lines indicate the angular position of the SVV for the upper left and the upper right gaze directions, respectively, assuming the complete lack of torsion compensation.

exceeded 6°, the monkeys reported the correct tilt direction in >90% of the trials and responded at chance level (50%) when the line tilt was around zero (*SI Appendix*, Fig. S2*B*). This chance-level point—the point of equal selection (PES)—served as a measure of the monkeys' subjective visual vertical (SVV) in the actual psychophysical experiment starting after several weeks of intensive training. Here we stopped presenting the visual reference line, assuming that the monkeys would now use an internal reference corresponding to their subjective vertical ("test trials"). The results described below support the conclusion that this was indeed the case. The monkeys were given a reward whenever they correctly reported the line tilt for angles exceeding 6° in either direction but were rewarded at random, independent of their perceptual decision, for angles smaller than 6°. The latter trials were always few (10 to 15%) and randomly interwoven into the other trials. SVV measurements were based on the test trials and were carried out for three different gaze positions: central (0°, 0°), upper right (20°, 20°), and upper left (−20°, 20°) with respect to straight ahead. These gaze positions were acquired by presenting the fixation point on one of three monitors, positioned tangentially on a virtual spherical surface (radius 107 cm) centered on the midpoint between the monkeys' eyes (Fig. 1*A*). When the monkeys gazed straight ahead, the SVV was 89.37° (95% confidence bounds [conf. b.] 89.36, 89.39) and 88.54° (88.5, 88.58) for M1 and M2, respectively, i.e., deviating marginally, yet significantly ($P < 0.005$, t test) from the world vertical (90°) in a cw direction (Fig. 1*B*). When the gaze was shifted to the upper left, the eyes rotated significantly ($P < 0.05$, t test) by 5.2° and 5.75° (95% conf. b. 4.6, 5.6 and 5.12, 6.38, pooled across days and both eyes for M1 and M2, respectively) ccw (*SI Appendix*, Fig. S3; see *SI Appendix* for details on the eye torsion measurements about the gaze axis relative to the eyes looking straight ahead). The SVV, on the other hand, displayed only a comparatively minor, yet significant change ($P < 0.05$) by 1.59° ccw to 90.96° (95% conf. b. 90.93, 90.97) for M1 and a relatively larger change by 3.96° ccw to 92.48° (95% conf. b. 92.52, 92.45) for M2. If the SVV had been referenced to the retina, one would have expected rotation of the SVV by an amount corresponding to the eye rotation and no change whatsoever in the case of a head- or world-centered reference system, requiring full compensation of eye torsion. The actually measured SVV reflected only partial compensation, taking into account 65% of the eye torsion in M1 and 31% in M2. When the gaze was shifted to the upper right, the eye torsion amounted to 5.5° and 6.45° (95% conf. b. 4.75, 6.25 and 5.5, 7.44 pooled across days and both eyes from M1 and M2, respectively) cw relative to straight ahead with respect to the central fixation ($P < 0.005$, t test). Again the SVV changed very little, yet significantly by 0.15° cw to 89.22° (conf. b. 89.2, 89.25 [$P < 0.005$ t test] relative to the gaze straight baseline) for M1 and by 2.88° cw to 85.79° (conf. b. 85.83, 85.74 [$P < 0.005$ t test]) for M2. Hence, whereas in M1 the perceived SVV indicated that a substantial, albeit not complete (97%) compensation of the perceptual consequences of the eye torsion for the SVV had taken place, the compensation in the case of M2 was substantially smaller (57%). Finally, when directly comparing the two eccentric gaze positions, the average difference in SVV orientations amounted

to 1.74° (conf. b. 1.56, 1.92) for M1 and 6.69° (conf. b. 6.65, 6.73) for M2, whereas the average difference in eye torsion was 10.2° (conf. b. 9.6, 10.8) for M1 and 12.2° (conf. b. 11.13, 13.27) for M2. In other words, the perceptual compensation of changes in eye torsion associated with fixation shifts from one eccentric position to the other amounted to 82% for M1 and to 45% for M2. The amount of compensation is in general on an order of magnitude comparable to the one reported for humans and it is important to note that also humans may exhibit considerable interindividual differences (4).

Differential Consideration of Eye Torsion by V1 Neurons. After having established that monkeys' perception of image tilts due to false torsion corresponds to that of humans, we embarked on a search for its neuronal correlate. To explain the percept, the neuronal correlate should reflect the extensive, yet not complete transformation of visual orientation responses from retinal into world-/head-centered coordinates based on the integration of information on false torsion. We assumed that this integration could take place already at the level of area V1 given the exquisite sensitivity of V1 neurons to the tiny changes in object image orientation and position resulting from false torsion.

To critically test this idea, we compared the RF positions and preferred orientations of V1 neurons for at least two and in many cases for all three gaze directions studied in the psychophysical experiment on the SVV.

Fig. 2 *A* and *B* depicts the orientation tuning curves of two exemplary V1 neurons that represent the diversity of responses to false torsion. Tuning curves were obtained by flashing Gabor gratings centered on the neuron's RF, whose orientation was varied at random in steps of 2°. The size and the spatial and temporal frequencies of the moving grating stimuli were adapted to the needs of the individual neuron (see *SI Appendix* for more details). The tuning curves in Fig. 2 *A* and *B* are plotted in a head-centered frame of reference (FOR) on the left and in a retina-centered FOR on the right. The neuron shown in Fig. 2*A* exhibited a tuning curve that stayed put when plotted in retinal coordinates, independent of the difference in eye torsion. In other words, this neuron showed behavior in accordance with the standard notion of retina-centered coding in V1. However, the neuron depicted in Fig. 2*B* presented a tuning curve that rotated on the retina by 9.42° (conf. b. 10.75, 8.09), i.e., relatively close to the false torsion difference measured in this particular session, which amounted to 11.7° (conf. b. 11.55, 11.85). Correspondingly, when plotted in head-centered coordinates, the orientation tuning curves did not change much with false torsion. We analyzed the dependence of the orientation preferences on the amount of false torsion associated with eccentric gaze in 114 neurons, 54 from M1 and 60 from M2, all having RFs in the lower left visual quadrant and most of them located in layers 2 and 3, based on the criteria of Snodderly and Gur (12) (*SI Appendix*, Fig. S4 *B* and *C*). To quantify changes in orientation preferences prompted by eye torsion we calculated an orientation updating index given by the inverted difference between preferred orientations in head-centered coordinates for two gaze directions divided by the associated amount of eye torsion change between the two (orientation updating index [OUI] = −1 × orientation change/eye torsion change). The angular change in preferred orientation from one gaze direction to another one was obtained by determining the location of the peak of the cross-correlation function between the individual tuning curves plotted in head-centered coordinates. The OUI is close to 0 for a neuron, which—like the one shown in Fig. 2*B*—is able to stabilize the orientation tuning curve relative to the head by largely compensating changes in eye torsion. It will be −1 for a neuron like the one shown in Fig. 2*A*, lacking any compensation of eye torsion, encoding the visual world in retina-centered coordinates (see *SI Appendix* for more examples; *SI Appendix*, Fig. S5*B*). OUIs larger than zero reflect overcompensation of eye torsion and OUIs smaller than −1 erroneous shifts of the orientation preference in a direction opposite to the one allowing compensation of eye torsion. Fig. 2*C* plots the distributions of the OUIs for M1 and M2. Individual OUI distributions were broad and unimodal (Hartigan's dip test; $P = 0.93$ and $P = 0.88$, for M1 and M2, respectively) with means of −0.21 and −0.41 for M1 and M2 that were significantly different from zero and not significantly different from each other ($P = 0.14$, Wilcoxon rank sum test). Hence, substantial variability notwithstanding, at least at the population level, in both monkeys, V1 neurons were able to correct for eye torsion-induced image tilt to a substantial degree. If V1 populations were responsible for compensating the influence of false torsion on perceived orientation, one would expect that average OUI for a certain amount of false torsion should predict changes of SVV for that condition. To test this expectation, we calculated a measure of perceptual compensation, the subjective visual vertical updating index (SVV_UI), given by the change of the SVV when shifting gaze from one position to another one, divided by the amount of associated false torsion change. As a matter of fact, the SVV_UI changed in the two monkeys similarly to changes of their respective OUI. SVV_UI in M1 had a mean of −0.18 (conf. b. −0.21, −0.15) that indicated a perceptual undercompensation of false torsion very close to M1's neural undercompensation as given by a mean OUI (mean) of −0.21 (conf. b. −0.29, −0.13). M2 exhibited a larger perceptual and as well a larger neural undercompensation with means of −0.41 (conf. b. −0.48, −0.33) and −0.38 (conf. b. −0.53, −0.22) for the SVV_UI and the mean OUI, respectively. In other words, the features of the perceptual updating of the SVV may be understood as reflections of changes in the orientation preferences of populations of V1 neurons.

Population Activity in V1 Reflects Perception of Orientation. To provide additional support for the notion that the population activity of V1 neurons can account for the perceptual compensation, we also compared normalized population orientation curves for the three gaze directions. Normalization was achieved by first scaling discharge rates for the various grating directions relative to the discharge rate for the preferred direction set to 1. Next, we rotated the orientation tuning function of a given neuron obtained for the central gaze direction such as to align the preferred direction of this neuron with the head-centered horizontal and rotated the same neuron's tuning functions for the eccentric gaze directions by the same amount (*SI Appendix*, Fig. S8). Fig. 3*A* depicts the resulting normalized population orientation tuning functions of each monkey for the three gaze directions on top of each other in a head-centered FOR. For the eye, the tuning curves associated with eccentric gazes stay relatively closely aligned with the head-centered horizontal. This is in accordance with the notion of a population-based encoding of visual orientation in a FOR close to head-centered FOR in V1, independent of gaze directions.

The notion of a close link between the orientation judgments and the properties of V1 neurons is also supported by the fact that the OUIs and the SVV_UIs change similarly with changes in gaze positions. For example, M1 exhibited the smallest SVV_UI for a gaze shift from the central gaze to the one on the upper right and the largest one for gaze shifts from the central gaze to the upper left gaze direction. Correspondingly also the OUI was smaller for the first condition and larger for the second one (Fig. 3 *B*, *Left*). In agreement with these observations on M1, M2 showed the smallest SVV_UI for gaze shifts from the central to the upper right gaze and, correspondingly, also the OUI was smallest for the change between these two gaze directions. Gaze shifts from upper left to upper right and from central to upper left directions had relatively large SVV_UI and OUIs that exceeded 0.5 for both (Fig. 3 *B*, *Right*). A final argument supporting the link between V1 population activity and the percept

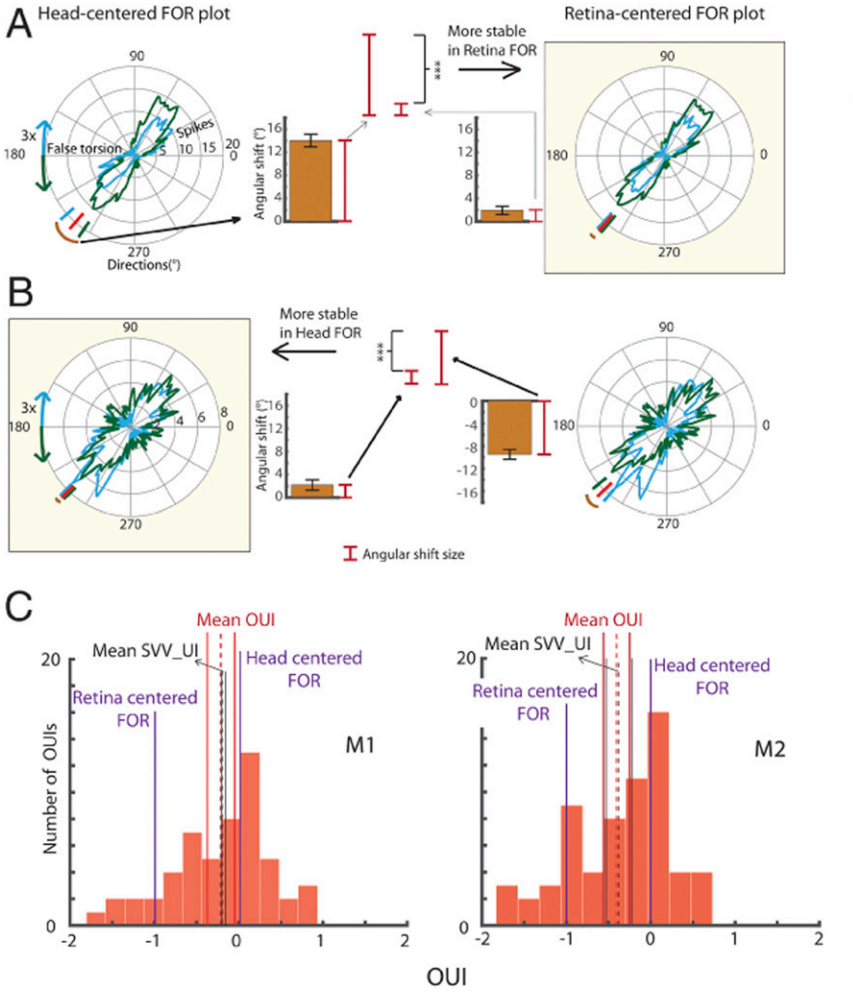

Fig. 2. Diverse effects of false torsion on orientation tuning curves of V1 neurons. (*A* and *B*) Superimposed orientation tuning curves of two exemplary neurons obtained with the monkey fixating either on the upper left gaze direction (data in green) or on the upper right one (data in blue). The angular axis represents the grating orientation and the radial axis the discharge rate evoked. In *A* and *B*, *Left* we plot the orientation tuning curves in a head-centered FOR and in *A* and *B*, *Right* we plot those in a retina-centered FOR. The green and blue arrows in the head-centered FOR plots mark off the difference in eye torsion between fixation on the upper left and right gaze directions. The small green, red, and blue lines perpendicular on the outer circle of the polar plots indicate the preferred grating orientation for the upper left, middle, and upper right gaze directions in the respective frame of reference (head-centered FOR on *Left*, retina-centered FOR on *Right*). The preferred orientation is perpendicular to the preferred direction of grating movement. The brown arc segments represent the angular difference between preferred orientations for the two. This difference is also reflected in the bar plot (mean ± SEM) next to the orientation tuning plot. The orientation preference of the neuron shown in *A* is more stable in a retina-centered FOR as the angular difference between preferred orientations is much smaller for this FOR than for the head-centered one. The reverse is true for the neuron shown in *B*. (*C*) Histograms of the OUIs of all neurons from each monkey, *Left* for M1 and *Right* for M2. Fully head-centered neurons have an OUI of 0, and those which are retina centered have one of 1. Note that each OUI represents pairwise comparisons between the tuning curves associated with two different gaze directions. Hence, if a neuron were tested for all three gaze directions (yielding three tuning curves), it would contribute to the histogram with three individual OUI values. The dashed and solid black vertical lines indicate the mean SVV_UI and their confidence boundaries for M1 and M2 based on pooling the data for all three gaze directions. The dashed and solid red vertical lines indicate the averages and confidence boundaries of OUI for M1 and M2. Note that SVV_UI and OUI are overlapping for M1 and that they are both shifted toward a retina-centered FOR for M2.

of the vertical is provided by a comparison of the two monkey individuals. As said earlier (Fig. 2*C*), the SVV_UIs associated with shifts of fixation were on average considerably smaller in M1 than in M2 ($P < 0.05$, t test). Accordingly, also the associated mean OUI changes were substantially smaller in M1 (–0.277; conf. b. –0.271, –0.283) than in M2 (–0.574; conf. b. –0.582, –0.566).

On closer inspection, the normalized population orientation curves shown in Fig. 3*A* suggest a better discrimination between the best and the worst orientation because of slightly larger responses for the best orientation (M1) or, alternatively, stronger suppression of responses for the orthogonal orientation (M2). This impression is supported by a quantitative comparison, based on an orientation sensitivity index (OS), which relates the discharge for the preferred orientation relative to the orthogonal one: OS = (preferred orientation − orthogonal orientation)/(preferred orientation + orthogonal orientation). For the data pooled from both monkeys, OS was indeed significantly larger for straight ahead with a mean of 0.56 (conf. b. 0.554, 0.566) than for the two other gaze directions (upper right mean of 0.54 and conf. b. of 0.534, 0.546; upper left mean of 0.52 and conf. b. of 0.516, 0.526). The same result was obtained when neurons from M1 and M2 were considered separately (Fig. 3*C*). Assuming that orientation judgments are based on a population vote of all neurons in V1, less sharp orientation tuning of the population responses for eccentric gaze should translate into less certain orientation judgements. This is exactly what the perceptual data

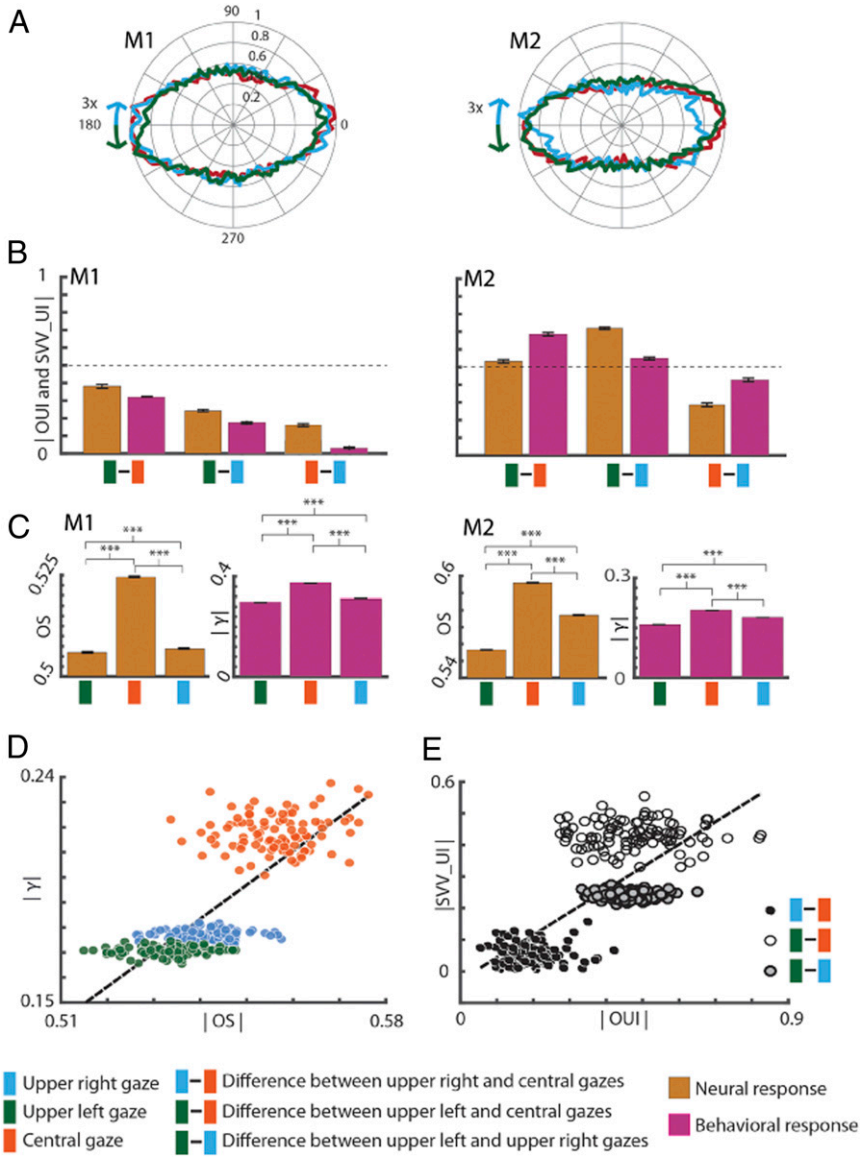

Fig. 3. Population activity in V1 predicts the eye position-dependent SVV shift. (*A*) Population tuning curves for the gaze directions for M1 and M2 with data for the eccentric gaze directions aligned with respect to the central one (see *SI Appendix* for details). Data for the upper right gaze direction are in blue, those for the upper left one are in green, and those for the central gaze direction are in red. (*B*) Bar charts comparing the pairwise OUIs (brown) based on the normalized population tuning curves for the three gaze directions in M1 and M2 with respect to SVV_UIs (pink). Bear in mind that we plot the absolute values of the OUIs and SVV_UIs. Note that the OUIs and SVV_UIs for M2 were larger than for M1. (*C*) Bar chart pairs plotting the mean orientation selectivity of the normalized population tuning curve (mean ± SE, brown; left part of each pair) and the absolute value of the steepness of the slope of the psychometric function (pink; right part of each pair) (parameter γ, see *SI Appendix*). Data based on all neurons from M1 are shown on *Left* and those from M2 are on *Right*. (*D*) Plot of the absolute values of γ against the absolute values of OS. The plot includes 300 data points, 100 for each gaze direction, where each data point was calculated in one iteration that selected 70% of the pooled data randomly chosen from M1 and M2. The correlation between γ and OS is significant ($r = 0.64$, $P < 0.0001$). (*E*) Plot of the absolute values of OUIs against the absolute values of SVV_UIs. The correlation between the OUIs and the SVV_UIs is significant ($r = 0.75$, $P < 0.0001$). The error bars indicate SE (***$P < 0.001$, *t* tests).

for monkeys M1 and M2 exhibited: As shown in Fig. 3*D* the steepness γ of the psychometric functions fitting M1 and M2 perceptual decisions around the point of equal selection was significantly less ($P < 0.001$, *t* test) for eccentric gaze than for gaze straight ahead.

To directly test whether the neural activity in V1 correlates with perceptual decisions on a tilted line in space, we performed a bootstrapping analysis based on pooled neural and perceptual data drawn in almost equal parts from both monkeys. We generated 100 OSs and γ values for each gaze direction using 70% (with replacement) of the data in each iteration. This resulted in 300 OSs and γ values for the three gaze directions, which were correlated with each other significantly ($r = 0.77$, $P < 0.0001$) (Fig. 3*D*). For the preferred orientation update analysis, we generated 100 OUIs for each pair of gaze directions (e.g., between upper right and central gaze directions) to end up with 300 OUIs and 300 SVV_UIs for the three possible combinations. OUIs correlated significantly with SVV_UIs ($r = 0.72$, $P < 0.0001$) (Fig. 3*E*), suggesting indeed a strong link between the activity in V1 and the perceptual decision on a tilted line.

We explored the eye torsion-dependent changes of the neuronal responses and their relationship to the perceptual

judgments further by modeling judgments based on the assumption that they reflect the integration of information on visual orientation and on eye torsion (Fig. 4*D*). The model (see *SI Appendix* for details) assumes that information on visual orientation is originally available in a retinal FOR. As the visual signal reflects the collective vote of a number of orientation-selective neurons tuned to individually different preferred orientations, the noise level should not depend on the specific orientation preference, for the sake of simplicity ignoring here the complication of the oblique effect (13–15). On the other hand, eye torsion-associated noise should grow with torsion as torsional information is assumingly conveyed by neurons encoding eye torsion in a monotonic format (10, 16, 17). This two-component model, fitted to the three psychometric curves, was able to reproduce the observed SVV associated with the three fixation positions very well ($r^2 = 0.99$ and 0.98 for M1 and M2, respectively; Fig. 4 *A* and *B*), including the perceptual undercompensation of false torsion and the lower γ of the psychometric functions for the eccentric fixation positions (Fig. 4 *C* and *E*). Assuming that the perceptual judgments are based on a V1 population vote, we suggest that the increase in eye position-dependent noise assumed in the model explains the poorer orientation sensitivity of the population response for eccentric gaze directions. The model prediction accommodates the tilting of the SVV by about 0.15° cw and 0.45° cw relative to the true vertical for M1 and M2, respectively, by assuming a torsional bias during straight ahead fixation (Fig. 4 *F* and *G* and *SI Appendix*, Fig. S9). This perceptual bias also contributes to the perceptual judgments for the eccentric gaze directions. Subtracting the eye torsional bias leads to tilts of the SVV that become much more mirror symmetric relative to the true gravitational vertical.

Vertical Visual Context Supports Perceptual Compensation of False Torsion. Our experiments were carried out in darkness and great care was taken to exclude any oriented visual landmarks, potentially serving as a reference for the perceptual interpretation of the oriented line. However, one might argue that inadvertent orientation cues, available only after some time of adaptation, cannot be excluded with absolute certainty. In this case, the relative insensitivity of orientation judgments to false torsion might be due to the visual context serving as reference rather than being a consequence of a torsion prior. On the other hand, a visual background, aligned with gravity and not tilted by false torsion, might provide the information needed to improve the perceptual reinterpretation of object orientation. Against this backdrop we asked whether a large vertical squared frame (19° × 19°) serving as a proxy of a natural visual background would influence perceptual decisions of M2 on line orientation. Assuming the absence of relevant orientation cues in our standard setting, we expected that the introduction of the visual background would render the perceptual judgments about line orientation even less dependent on false torsion. This was indeed the case. Changing the fixation position from one gaze direction to another and thereby the torsional state of the eyes caused

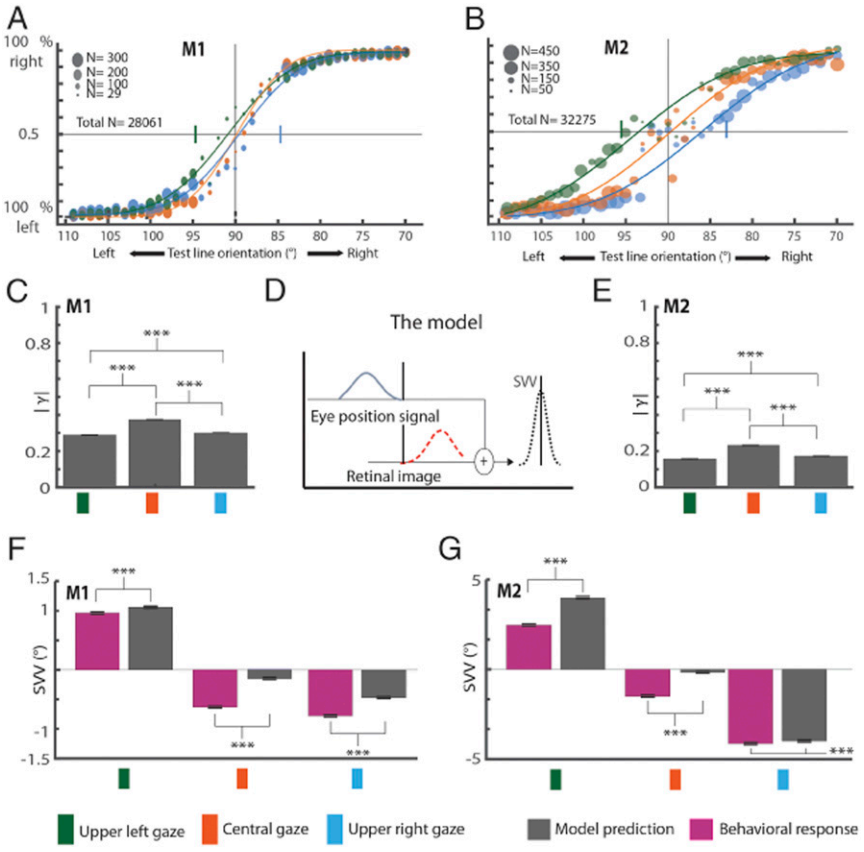

Fig. 4. Modeling the SVV based on the integration of visual information and an eye torsion prior. *A* and *B* plot fits of the function derived from the Bayesian model to the psychophysical data on the SVV of M1 and M2. The red, blue, and green colors distinguish experimental data and model predictions for the three gaze directions. (*C* and *E*) Bar chart summarizing the |γ| values of the psychometric functions (means ± SE) predicted by the Bayesian model for the three gaze directions. Note that the predicted |γ| shows a dependence on the gaze direction similar to the gaze direction dependence of the measured |γ| shown in Fig. 3*C*. (*D*) Sketch of the model structure. (*F* and *G*) Bar charts indicating the measured SVV (pink) and the SVV estimated by the model (dark gray) for the three gaze directions. Note that the model was able to predict the direction and relative amount of error of SVV across gaze directions quite well (***$P <$ 0.001, *t* tests).

significantly smaller changes of the SVV when the visual frame was available compared to when it was not ($P < 0.05$, t test; corrected for multiple comparisons using false discovery rate correction) (18). However, the SVV was not perfectly vertical as it deviated from the true vertical by 1.18° cw (conf. b. 1.13, 1.24) for the central monitor, by 2.09° cw (conf. b. 2.05, 2.14) for the upper right monitor, and by 2.48 ccw (conf. b. 2.45, 2.52) for the upper left monitor ($P < 0.05$, t test; corrected for multi-comparisons) (Fig. 5 *A* and *B*). As expected, given the availability of additional information on the true vertical, orientation judgments became more precise compared to the standard setting as indicated by steeper psychometric functions for all three fixation positions (Fig. 5*C*) with the expected decrease. The fact that also in the presence of the visual reference, the precision of decisions for the eccentric fixations was significantly less than that for straight ahead indicates that nonvisual information on eye torsion matters also in the presence of a visual reference on the true vertical. We considered two variants of the original model to evaluate the influence of eye torsion on the orientation decision in the presence of the frame. The first model relied solely on the visual background as a reference for the world vertical and ignored the eye torsion relative to the world. The second one corresponded to the original model, deploying nonretinal information on eye torsion to correct for the retinal image tilt, now with the additional consideration of the visual background-based reference (*SI Appendix*, Fig. S10 *A* and *B*). Both models predicted the psychophysical data on the SVV well, collected in the presence of the frame. Yet, the consideration of eye torsion information, the characteristic of model 2, was needed to account for the poorer decision precision for the eccentric gaze directions (*SI Appendix*, Fig. S10).

V1's RFs Account for False Torsion. Torsional eye movements not only rotate the object image relative to the retinal meridian but also translocate the image if located outside the center of rotation. To ensure spatial stability, the RFs underlying the representation of the object should move relative to the retina in a fully compensatory manner. For 99 of them, 52 from M1 and 47 from M2, we were able to obtain detailed RF maps by resorting to a reverse correlation approach (*SI Appendix*) not only for the straight ahead eye position but also for at least one of the two eccentric gaze directions, in many cases for both (*SI Appendix*, Fig. S4*A* and Fig. 6 *A* and *B*). We quantified how much the angular position of RFs changed with eye torsion by calculating a RF updating index (RFUI) (RFUI = −RF angular position change/eye torsion change). A RFUI of −1 indicates retina-centered RFs and a RFUI of 0 head-centered coding, i.e., an updating of receptive field position by fully considering the amount of gaze direction-dependent eye torsion. The resulting distribution of RFUIs (Fig. 6*C*) pooled over data from M1 and

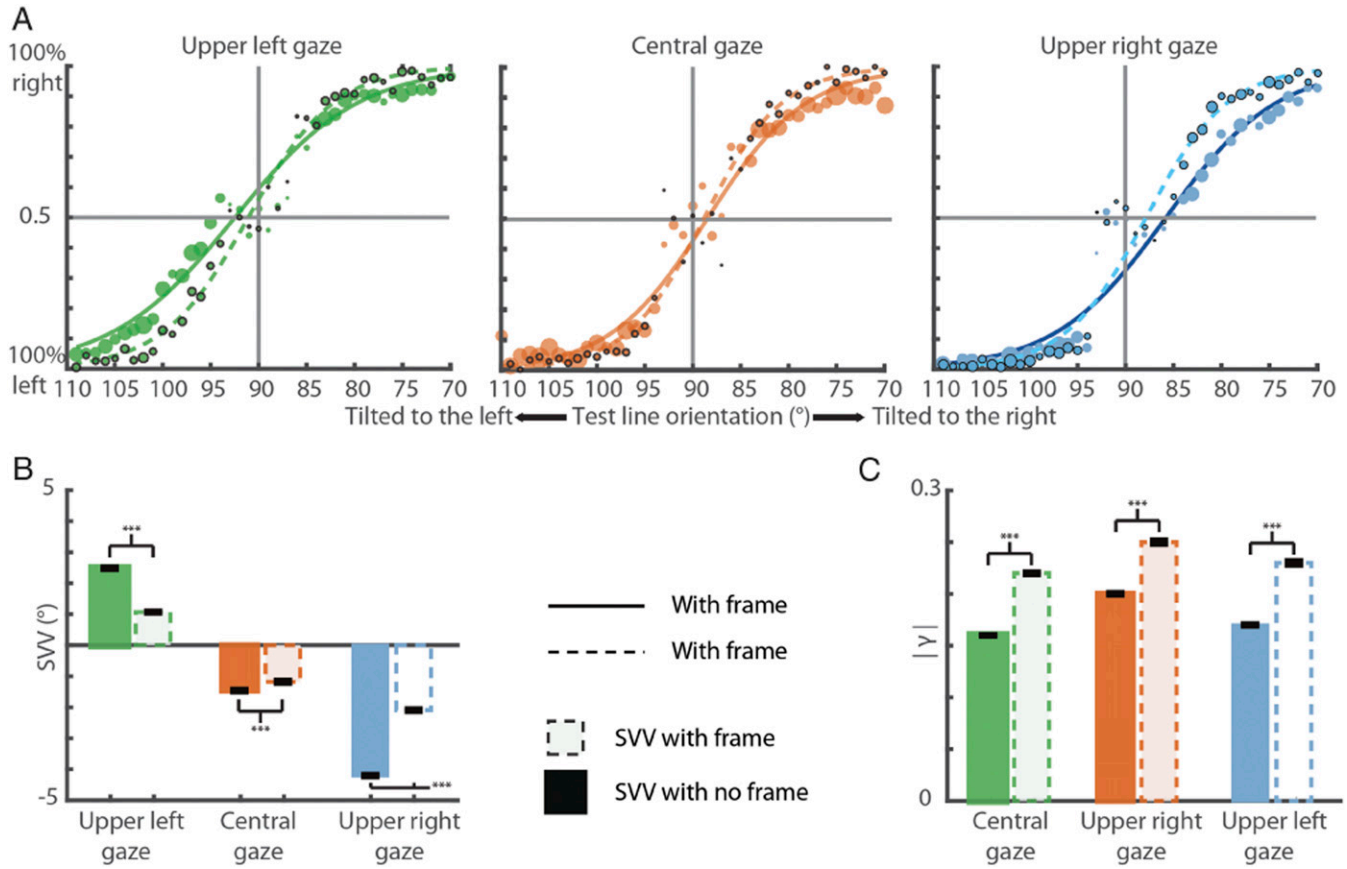

Fig. 5. The role of a visual reference in the compensation of false torsion. *A* plots psychometric functions fitting the orientation decisions for all three gaze directions. The red, blue, and green colors distinguish data for fixation on the central, the upper right, and the upper left gaze direction, respectively. The circles with black boundaries represent data collected with a visual frame present on the monitor and the circles without boundaries show data collected with no frame. Dashed and solid curves represent the psychometric functions fitted to the data collected with frame and without frame, respectively. (*B*) Bar chart plotting the SVV deviation from the true vertical (mean ± conf. b.) with the solid bars representing the deviation in the absence of a frame and the bars with dashed boundaries the deviation measured in the presence of the frame. Note that the deviation is significantly less when presenting the frame (***$P < 0.001$, t test). (*C*) Bar chart plotting the steepness |γ| of the psychometric function for each gaze direction with (solid bars) and without (dashed bars) frame. Note that |γ| values increase when the frame was presented, indicating higher precision of decisions on line orientation (***$P < 0.001$, t test).

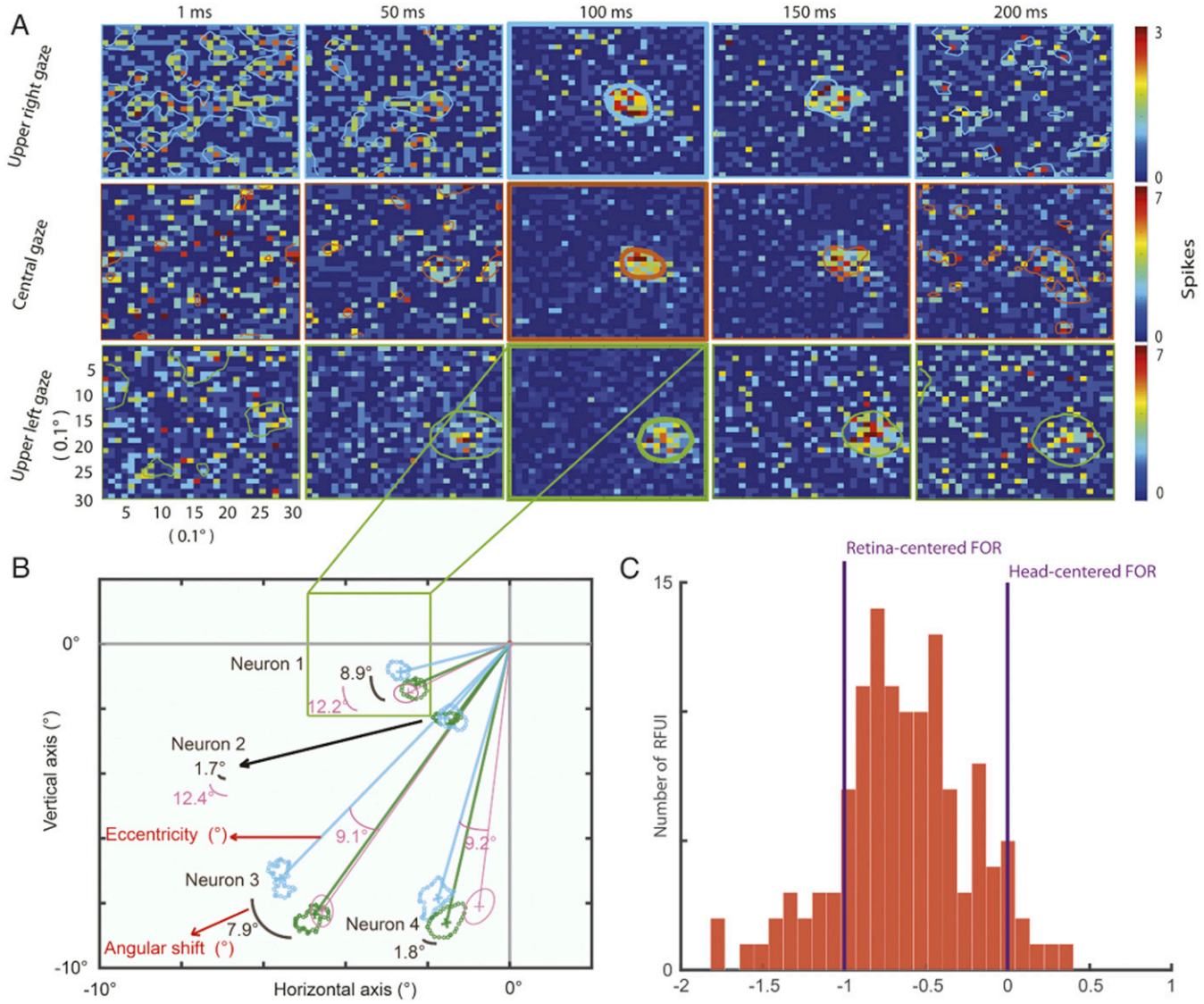

Fig. 6. The impact of false torsion on the RF positions of V1 neurons. (*A*) RF maps of an exemplary V1 neuron ("neuron 1") at different times relative to stimulus onset ($t = 0$ ms) as revealed by reverse correlation. Plots are in head-centered coordinates and the three rows depict the maps obtained for the three gaze directions (i.e., fixation on the upper left, the central, and the upper right gaze direction). The maps highlighted by thick colored contour lines represent the peak responses. The peak response and the time of its occurrence were determined by summing all spikes along the *y* dimension, giving a one-dimensional vector of elements presenting the number of spikes along the *x* dimension. The time relative to stimulus onset yielding the *x* vector with the largest peak was then taken as the time of the peak response. The thick colored contour lines demarcate the boundaries of the RFs at the time of the peak response. The contours obtained for the two eccentric gaze directions are reproduced in the visual field map with respect to the fixation point depicted in *B*. (*B*) This map compares the RFs of neuron 1 and three others in a head-centered FOR for fixation in the two eccentric gaze directions. RFs for gaze shifted to the upper right are shown in blue, and those for gaze to the upper left are in green. In addition, the RF positions for gaze in the upper left direction to be expected if neurons used a purely retina-centered FOR are indicated by schematic elliptic RF boundaries (pink). The dark brown arc segments display the effective angular shift of RFs in head-centered coordinates (numbers attached), whereas the pink arc segments indicate the difference in false torsion. Note that the eccentricity is the distance between the RF and fixation point as indicated by the red arrow. (*C*) Histogram of the RFUI = RF shift/torsional eye shift of all neurons collected from M1 and M2 pooled. Note that individual neurons may contribute one or three RFUIs, depending on whether RF maps were obtained for two or three gaze directions.

M2 is broad and unimodal (Hartigan's dip test; $P = 0.94$) with most values located between RFUI of 0 and −1. This is in line with the OUI distribution which was unimodal and broad as well. Note that these results cannot be influenced by possible differences in the quality of fixation for the three gaze directions as there were none: When plotted in monitor coordinates, the mean fixation positions for the three gaze directions were the same for eye position data sampled together with the neuronal data (Kruskal–Wallis ANOVA with the factor gaze direction, $P = 0.12$ and $P = 0.39$ for horizontal eye position for M1 and M2, respectively, and $P = 0.11$ and $P = 0.39$ for vertical eye position for M1 and M2, respectively). Also, the eye position variance for the three gaze directions did not differ significantly ($P = 0.14$ for M1 and $P = 0.37$ for M2). Gaze direction-dependent changes in eye torsion affected the angular position of RFs, yet did not change their eccentricity. Accordingly, we did not find any change in the mean eccentricity of RF locations with gaze direction (*SI Appendix*, Fig. S11*A*). Finally, gaze direction-dependent changes in eye torsion can be expected to affect the orientation preference and the angular position of its RF in a

yoked manner. That this is indeed the case is supported by the fact that the amount of RF updating correlated significantly with the orientation preference shifts recorded from the same neuron (*SI Appendix*, Fig. S11*B*).

Discussion

Donder's law alleviates the control of exploratory eye movements by reducing the degrees of freedom from three to two by specifying the amount of eye torsion associated with any x, y eye position (1, 2, 19). By the same token, Listing's law alleviates the perceptual interpretation of retinal image orientation by constraining eye torsion—and consequently the amount of image torsion relative to the retinal meridian—to just one value, firmly and reliably associated with a given x, y eye position (1, 2). The prior knowledge of this value, the amount of false torsion, allows a transformation of the retinal image, tilted by a small, yet significant amount for eccentric gaze, into a new FOR that is rotated relative to an eye-centered FOR such as to minimize the influence of eye torsion on the visual representation. Our study shows that information on false torsion is taken into account at the level of area V1, allowing V1 to make possible a representation of object orientation that is independent of eye gaze direction-induced torsion. Perceptually, false torsion is compensated largely, but not completely. The fact that the amount of perceptual undercompensation is predicted by the collective orientation vote of V1 neurons supports the notion that it is V1 that allows us to cope with the perceptual consequences of Listing's law. A simple Bayesian model of orientation judgments, integrating information on visual orientation of the test line and false torsion, suggests that the advantage of tolerating this small amount of undercompensation might be to limit the impact of eye position-dependent noise, more and more influencing perceptual judgments for larger amounts of eye torsion. Previous work (10, 16, 20–23) supports our model assumption that eye position and eye torsion are encoded in a monotonic format, no matter whether the basis of the position signal is proprioceptive feedback or efference copy, i.e., a torsion prior. While we cannot exclude that the signal on eye position used by V1 has a proprioceptive nature, we think that the usage of a torsion prior would have the advantage of avoiding delays, allowing a prediction of the sensory consequences of torsion ahead of the movement.

False torsion influences not only image orientation but also image position on the retina. As we are lacking reliable information on the influence of false torsion on the perception of image position, it must remain open whether the RF position shifts observed are able to explain the percept. As the population data indicate that torsion-induced changes in object position are on average compensated only about half, one might also expect that the degree of perceptual position invariance may be substantially less than the perceptual orientation invariance. On the other hand, the evidence for a subgroup of neurons with almost perfect eye torsion invariance of RF positions may on the contrary suggest perfect torsion invariance, assuming that only this subgroup underlies the percept. However, this does not seem to be likely when considering that also orientation judgments were much better explained when considering the whole population of neurons, not only those found in the distribution mode comprising largely torsion-invariant neurons. Actually, the scarce perceptual data on humans might be taken to suggest that subjects partially misjudge the position of a flashed probe with respect to the head plane during eccentric fixation (6), supporting the assumption of a collective neuronal vote.

The perceptual compensation of false torsion demonstrated in our experiments was substantial, yet not complete, which is why one might expect that the percept of the orientation of the visual world might be compromised. Yet, already the introduction of a simple visual frame as proxy of a visual background, providing supportive information on the world vertical, was able to substantially reduce the perceptual undercompensation. Hence, arguably a richer visual background available under conditions of natural vision may further reduce the undercompensation to an extent rendering it virtually unperceivable. Where and how the visual and the nonvisual information on the world vertical get integrated is a matter of speculation.

The fact that V1 takes information on eye torsion into account to minimize the consequences of false torsion for the perception of object orientation and position does not necessarily imply that V1 encodes visual information in a fully head-centered frame of reference, i.e., also minimizing the horizontal and vertical deviations of the eyes relative to the head. False torsion due to Listing's law is not the only form of eye torsion whose perceptual consequences are compensated by V1. Another form is ocular counter roll evoked by tilting the head about the roll axis. A specific subset of V1 neurons uses information on counter roll to render visual orientation and position in a head-centered FOR, thereby helping to establish a world-centered representation of the visual world, invariant to roll tilt of the head and body (24). As ocular counter roll is small, its contribution to a tilt-independent percept of the vertical is negligible. In fact, the generation of a tilt-invariant representation would be simplified considerably if the ocular counter-roll response to head tilt would be simply vetoed, making the consideration of eye torsion dispensable. Why is this not the case? The answer may be that perfect vetoing of counter roll, a phylogenetic vestige of lateral-eyed ancestry, may simply be unnecessary. Counter roll is reduced by just an amount needed to make use of the machinery that is in any case required to cope with the consequences of false torsion.

Materials and Methods

Subjects. Two adult male rhesus monkeys (*Macaca mulatta*) took part in this study (M1, 10 y old, and M2, 8 y old). The experiments were approved by the local authorities in charge (Regierungspräsidium Tübingen and Landratsamt Tübingen), conducted in accordance with German and European law and the Guidelines of the National Institutes of Health for the Care and Use of Laboratory Animals and carefully monitored by the veterinary service of Tübingen University. A magnetic scleral search coil was implanted into the right eye to record two-dimensional (2D) eye position and a titanium head post was implanted to painlessly immobilize the head during experiments. We refrained from trying to document also torsion with search coils as we were concerned that the much bulkier 3D search coils might have a mechanical impact on the torsional eye position associated with eccentric fixation. Therefore, torsion was measured by comparing video images of the eyes acquired during stable fixation of the target presented in the center of the monitors. Six cameras were used, two for each monitor, in each case one for each eye, to guarantee an optimal alignment with the line of gaze of both eyes when the monkey fixated on the center of a particular monitor, thereby minimizing image distortion. We implanted a circular titanium chamber over the occipital cortex for electrophysiological recordings. All surgical procedures were conducted adopting aseptic techniques under adequate anesthesia consisting of isofluorane supplemented with remifentanil (1 to 2 $\mu g \cdot kg^{-1} \cdot min^{-1}$). All relevant physiological parameters such as body temperature, heart rate, blood pressure, pO_2, and pCO_2 were continuously monitored. Postoperatively, buprenorphine was given until no sign of pain was left. Animals were allowed to fully recover before starting the experiments.

Single-Unit Recording. Extracellular action potentials were recorded with commercial glass-coated microelectrodes (Alpha Omega Engineering; impedance at 1 kHz, 0.5 to 1 MΩ). We inserted the electrode through the intact dura. We stopped advancing the electrode when it reached the brain and left it at that position for around 30 min to give the tissue a chance to relax after the penetration. Thereafter, we advanced very slowly (1 mm/h) to give the tissue sufficient time to adjust to the pressure exerted by the electrode. The position of a neuron relative to the top of cortex was estimated as the difference between the electrode position when recording the neuron's action potential and the electrode position at which we observed the last neural activity when later extracting the electrode again. This estimate, the

level of spontaneous activity of neurons at a given level, spike morphology, the preponderance of orientation versus direction selectivity, and other criteria suggested by Snodderly and Gur (12) were used to estimate the layer of a recorded neuron. Spikes of well-isolated single neurons were discriminated online by real-time sorting software based on template matching (Alpha Omega Engineering).

Experimental Setup and Behavioral Task. Three monitors (20° × 40°) were positioned tangentially on a virtual spherical surface (radius 107 cm) centered on the midpoint between a monkey's eyes. The central monitor was centered on the normal vector on the midpoint of the line, connecting a monkey's two eyes, taken as straight ahead (0°, 0°). The upper left monitor was centered at 20° left, 20° upward relative to straight ahead and the upper right monitor at 20° right and 20° upward. The alignment of the screens perpendicular to the line of sight was achieved by positioning a laser pointer in the monitor's center with the laser oriented perpendicular to the screen such that the laser hit the midpoint between a monkey's eyes. This allowed us to ensure that the monitor surfaces were aligned tangentially on a virtual sphere centered on the midpoint between a monkey's eyes. Consequently, the surface of the central monitor was oriented parallel to the gravity vector, whereas the surfaces of the eccentric monitors, displaced up relative to the central one, were tilted by about 20°. To ensure that the roll axes of the monitors were parallel to the horizon, we relied on information provided by an accelerometer system attached to the monitors (Analog Devices Inc.; dual axis accelerometer ADXL203EB), allowing us to sense misalignments at a resolution of ±0.1°. Importantly, the alignment of monitors was checked and—if necessary—adjusted before each experiment. We measured the monkeys' horizontal and vertical eye positions using a self-made search eye coil system supporting a sampling rate of 1,000 samples per second. The search coil signal was calibrated using the known position of a white fixation target dot (diameter 0.48°) that appeared at random on the monitor in one of nine positions defining a 3° × 3° grid centered on the monitor. Monkeys were asked to maintain fixation at each target for ∼1 s to get a liquid reward and then to proceed to the next cued location. Targets were visible for 2 s and had to be fixated successfully at least three times. The data acquired were subjected to a regression analysis that considered linear, quadratic, and mixed term dependencies to predict eye position based on the search coil voltage. To characterize the features of a neuron, after successful calibration the monkeys had to fixate on the target (diameter = 0.03) presented in the center of the central monitor for at least 10 min in total to allow us to map their RF and to assess their orientation preference. The background luminance was kept low (3 cd/m^2) to render constructive elements of the setup invisible as much as possible. On the other hand, it was high enough to guarantee photopic vision. Scotopic or mesopic vision would be deleterious as they entail quite variable luminance-dependent shifts of the retinal location preferred for fixation away from the fovea (25). Avoiding this instability of fixation was essential to map the small receptive fields, requiring that foveal gaze stayed reliably within a 1°-fixation window for at least 3 s. The monkeys were rewarded with a drop of juice or water, depending on individual preferences. Responses to visual stimulation were considered only if the aforementioned fixation requirement was met. Following testing visual stimuli on the central monitor, monkeys were required to fixate on the same target presented on the eccentric monitors, one after the other in pseudorandom order across days to rerun the analysis of neuronal response features.

SVV Task. The visual stimuli were presented within circular dark apertures (diameter = 16.5° without background frame and diameter = 20° with background frame), centered on the monitors, to prevent M1 and M2 from using the orientation of the monitor edges when judging the visual vertical (Fig. 1*A*). M1 and M2 were trained to report the orientation of a tilted line with respect to the head/gravity vector. A trial started with a period in which the monkeys had to fixate on a central dot (radius size 0.03°, fixation window 1°) for 800 ms, and next a line (7° visual angle length, 0.8° width) with varying orientation was added, whose lower end was centered on the fixation dot. Continued fixation was required. After 1 s, this "test" line and the fixation dot disappeared and two targets, left and right respectively of the monitor center, appeared for 700 ms asking the monkeys to make a saccade to one of them, depending on the perceived orientation of the line. After that, a bright homogenous background was introduced for 500 ms to erase the afterimage of the line. The left target was associated with ccw line tilts relative to the gravitational vertical and the right one with cw tilts. In the beginning of the experiment, a reference line (16.5° length and 0.8° width) indicating the gravitational vertical was available throughout the trial to help the monkeys understand the relationship between the test line tilt direction and the two response targets. In these training sessions, in which stimuli were usually presented only on the central monitor (*SI Appendix*, Fig. S2), the monkeys' performance was excellent (>90%) for tilt angles of 6° or larger. For smaller tilt angles the accuracy of judgments decreased proportionally with the decrease in tilt angle until it reached the level of chance performance (50%) for line tilts very close to zero (*SI Appendix*, Fig. S1*B*). At this point of subjective equality (PSE) the monkeys obviously guessed, as they were no longer able to detect a consistent tilt. After several weeks of training we started presenting the test line without the reference line in test trials randomly interleaved with the training trials (see *SI Appendix*, Fig. S2 for information on proportions) since the monkeys seemed to have understood the need to base tilt decisions on a more general concept of the vertical. Whereas in the training trials the monkeys were rewarded for correct choices, in the test trials a reward was given for correct choices in trials with tilt angles (relative to the gravitational vertical) exceeding >6° to either side as the monkeys did not have any problems in detecting the true tilt direction, even though the reference line was missing. For smaller tilt angles <6°, rewards were provided at random on average in 50% of trials, independent of choices to avoid the development of superstitious behavior, given the absence of clearly suprathreshold information on line orientation. There were always only a few trials with smaller tilts (10 to 15% of the test trials) to ensure that the monkeys' concept of an association of decisions (and rewards) on perceived line tilt would not be jeopardized. After several days, training trials could be fully omitted as M1 and M2 responses to test trials suggested reliable perceptual reports of SVV (*SI Appendix*, Fig. S2*A*). At this point, we also started to test the monkeys with stimuli presented on eccentric monitors. Responses were collected in blocks, usually starting with the stimuli presented on the central monitor, followed by the eccentric ones, pseudorandomizing the order of the upper left and the upper right monitors (Fig. 1*A* and *SI Appendix*, Fig. S2 *C* and *D*). The PSE was determined by fitting a psychometric function $\left(\frac{1}{1+e^{\gamma(\text{line tilt}-c)}}\right)$ to the test trial data, pooled across all sessions, independent of whether interleaved training trials had been presented or not. In this function, c is the line tilt angle (c) for which the function predicted a PSE and the parameter γ determines the steepness of the function at the PSE. The PSE served as an estimate of the monkeys' SVV in the absence of a visual reference.

Data Availability. Data for this article have been deposited in Figshare: https://doi.org/10.6084/m9.figshare.12159537.v1

ACKNOWLEDGMENTS. We are grateful to Friedemann Bunjes and Peter W. Dicke for technical support. We thank Nabil Daddaoua for his advice and comments. This work was supported by the German Research Foundation (Deutsche Forschungsgemeinschaft) Grant FOR 1847-A3 (TH 425/13-1), received by P.T. within the framework of the Research Unit "Primate Systems Neuroscience," and the Werner Reichardt Centre for Integrative Neuroscience, an excellence cluster grant received by the University of Tübingen (DFG EXC 307), coordinated by P.T.

1. D. Tweed, W. Cadera, T. Vilis, Computing three-dimensional eye position quaternions and eye velocity from search coil signals. *Vision Res.* **30**, 97–110 (1990).
2. H. H. von Helmholtz, *Handbuch der Physiologischen Optik*, (Leopold Voss, Leipzig, 1867).
3. G. Westheimer, Kinematics of the eye. *J. Opt. Soc. Am.* **47**, 967–974 (1957).
4. K. Nakayama, R. Balliet, Listing's law, eye position sense, and perception of the vertical. *Vision Res.* **17**, 453–457 (1977).
5. W. Haustein, H. Mittelstaedt, Evaluation of retinal orientation and gaze direction in the perception of the vertical. *Vision Res.* **30**, 255–262 (1990).
6. E. Poljac, M. J. M. Lankheet, A. V. van den Berg, Perceptual compensation for eye torsion. *Vision Res.* **45**, 485–496 (2005).
7. S. C. Goonetilleke, L. E. Mezey, A. M. Burgess, I. S. Curthoys, On the relation between ocular torsion and visual perception of line orientation. *Vision Res.* **48**, 1488–1496 (2008).
8. T. Haslwanter, D. Straumann, K. Hepp, B. J. M. Hess, V. Henn, Smooth pursuit eye movements obey Listing's law in the monkey. *Exp. Brain Res.* **87**, 470–472 (1991).
9. B. J. M. Hess, Three-dimensional visuo-motor control of saccades. *J. Neurophysiol.* **109**, 183–192 (2013).
10. J. Van Opstal, K. Hepp, Y. Suzuki, V. Henn, Role of monkey nucleus reticularis tegmenti pontis in the stabilization of Listing's plane. *J. Neurosci.* **16**, 7284–7296 (1996).
11. E. M. Klier, H. Wang, J. D. Crawford, Three-dimensional eye-head coordination is implemented downstream from the superior colliculus. *J. Neurophysiol.* **89**, 2839–2853 (2003).
12. D. M. Snodderly, M. Gur, Organization of striate cortex of alert, trained monkeys (Macaca fascicularis): Ongoing activity, stimulus selectivity, and widths of receptive field activating regions. *J. Neurophysiol.* **74**, 2100–2125 (1995).

13. A. R. Girshick, M. S. Landy, E. P. Simoncelli, Cardinal rules: Visual orientation perception reflects knowledge of environmental statistics. *Nat. Neurosci.* **14**, 926–932 (2011).
14. B. Chapman, T. Bonhoeffer, Overrepresentation of horizontal and vertical orientation preferences in developing ferret area 17. *Proc. Natl. Acad. Sci. U.S.A.* **95**, 2609–2614 (1998).
15. P. Vázquez, M. Cano, C. Acuña, Discrimination of line orientation in humans and monkeys. *J. Neurophysiol.* **83**, 2639–2648 (2000).
16. X. Wang, M. Zhang, I. S. Cohen, M. E. Goldberg, The proprioceptive representation of eye position in monkey primary somatosensory cortex. *Nat. Neurosci.* **10**, 640–646 (2007).
17. J. de la Rocha, B. Doiron, E. Shea-Brown, K. Josić, A. Reyes, Correlation between neural spike trains increases with firing rate. *Nature* **448**, 802–806 (2007).
18. D. Yekutieli, Y. Benjamini, Resampling-based false discovery rate controlling multiple test procedures for correlated test statistics. *J. Stat. Plan. Inference* **84**, 139–158 (2000).
19. F. C. Donders, Beitrag zur Lehre von den Bewegungen des menschlichen Auges. *Holl. Beitr. Anat. Physiol. Wiss* **1**, 104–145 (1848).
20. J. D. Crawford, T. Vilis, Symmetry of oculomotor burst neuron coordinates about Listing's plane. *J. Neurophysiol.* **68**, 432–448 (1992).
21. C. Helmchen, H. Rambold, L. Fuhry, U. Büttner, Deficits in vertical and torsional eye movements after uni- and bilateral muscimol inactivation of the interstitial nucleus of Cajal of the alert monkey. *Exp. Brain Res.* **119**, 436–452 (1998).
22. T. Villis, K. Hepp, U. Schwarz, V. Henn, On the generation of vertical and torsional rapid eye movements in the monkey. *Exp. Brain Res.* **77**, 1–11 (1989).
23. C. Helmchen, H. Rambold, U. Büttner, Saccade-related burst neurons with torsional and vertical on-directions in the interstitial nucleus of Cajal of the alert monkey. *Exp. Brain Res.* **112**, 63–78 (1996).
24. N. Daddaoua, P. W. Dicke, P. Thier, Eye position information is used to compensate the consequences of ocular torsion on V1 receptive fields. *Nat. Commun.* **5**, 3047 (2014).
25. O. Spivak, P. Thier, S. Barash, Monkeys use the rod-dense retinal region rather than the fovea to visually fixate small targets in scotopic vision. *bioRxiv*:10.1101/290759 (28 March 2018).